SIAM J. APPL. MATH.
Vol. 0, No. 0, pp. 000–000

UNIVERSAL STABILITY PROPERTIES FOR MULTILAYER HELE-SHAW FLOWS AND APPLICATION TO INSTABILITY CONTROL*

PRABIR DARIPA† AND XUERU DING‡

Abstract. With the motivation of understanding the effect of various injection policies currently in practice for chemical enhanced oil recovery, we study linear stability of displacement processes in a Hele-Shaw cell involving injection of an arbitrary number of fluid phases in succession. This work mainly builds upon our earlier study of the three-layer case [P. Daripa, *Phys. Fluids*, 20 (2008), 112101]. Stability results obtained for an arbitrary number of displacing fluids in succession reduce to the Saffman–Taylor case when there is only one displacing fluid. The stability results have been applied here to design injection policies that are considerably less unstable than the pure Saffman–Taylor case. In particular, two sets of parameters have been obtained that improve stability. Implementation of such injection policies based on the application of the stability results is likely to improve oil recovery.

Key words. hydrodynamic stability, Saffman–Taylor instability, linear stability, chemical enhanced oil recovery

AMS subject classifications. 76E17, 76S05, 76T99

DOI. 10.1137/11086046X

1. Introduction.

The displacement of a more viscous fluid by a less viscous one is known to be potentially unstable in a Hele-Shaw cell. Such flows, first studied by Hele-Shaw [14], are known as Hele-Shaw flows and have similarities with porous media flows [2] in the sense that in both of these flows, fluid velocity is proportional to the pressure gradient. Because of this analogy and the relative ease and accuracy with which such Hele-Shaw flows can be experimentally studied in comparison to flows in porous media, Hele-Shaw flows have been studied extensively over many decades. The instability theory in this context, also known as the Saffman–Taylor instability [23], is now well developed for single-interface flows. Exact growth rates of interfacial disturbances for such flows are well known and well documented in standard textbooks on hydrodynamic stability theory, e.g., Drazin and Reid [10].

Exact known stability results from these past works (see also formulas (1) and (2) in section 2) imply that increasing the interfacial tension suppresses instability, whereas increasing the positive viscosity-jump at the interface in the direction of flow further enforces instability [10]. Based on this understanding, it is common practice to use a layer of a third fluid with properties that are in between having viscosity less than that of the displaced fluid and more than that of the displacing fluid, in the hope that it will suppress the growth of instability that is otherwise present in the absence of this middle layer [25], [28], [24]. This expectation is justified based on the application of our understanding of single-interface flows to the multi-interface case under the assumptions that (i) the effect of interfacial interactions is negligible, and

*Received by the editors December 27, 2011; accepted for publication (in revised form) July 20, 2012; published electronically DATE. This work was supported by the Qatar National Research Fund (a member of The Qatar Foundation).
http://www.siam.org/journals/siap/x-x/86046.html
†Corresponding author. Department of Mathematics, Texas A&M University, College Station, TX 77843-3368 (daripa@math.tamu.edu).
‡Department of Petroleum Engineering, Texas A&M University at Qatar, Doha, Qatar (dxueru@gmail.com).

(ii) interfacial tensions at two interfaces are similar to the interfacial tension at the original interface between the displaced and the displacing fluid in the absence of the middle layer. This makes each of these interfaces less unstable individually due to reduction in the viscosity-jump across them. However, when interfacial tensions, as well as viscosity-jumps at two interfaces, are significantly modified due to the middle layer fluid, it is not easy to correctly predict the outcome of these collective effects on the overall instability of these flows from simple extrapolation of our understanding of single-interface flows. This problem becomes even more daunting in case of flows with an arbitrary number of interfaces.

Such flows involving an arbitrary number of interfaces arise during various flooding schemes in chemical enhanced oil recovery, a subject of intense current interest due to rising energy demands worldwide in a market of tight supply. To alleviate this situation, there is ongoing much needed research in the energy resources area. One such energy resources area is oil recovery. A fractional increase in the rate of oil recovery from an oil field using new oil recovery technology or even smarter use of existing technology will have a significant impact worldwide. Economic and geological uncertainties play a critical role in deciding the producing life of an oil field. Although there may still be producible oil in a field, economics of water handling and geological uncertainty of permeability fields and, to a lesser extent, porosity fields make producing the remaining oil economically very arduous. Currently, early water breakthroughs (which exacerbate the economics) limit oil recovery ranging from 10% to 35% depending on the type of reservoir. Typically, after primary production a waterflood is employed for pressure support and to further sweep away any oil that is left over, thus decreasing the field oil saturation. However, one potential drawback of the waterflood is the inability to accurately sweep away the oil due to an inadequate mobility ratio. Because of this drawback, it is estimated that total residual oil in matured reservoirs (reservoirs after conventional primary and secondary oil recovery) worldwide is around 70% of the original oil in place (OOIP). Therefore, it is important to investigate other alternatives to a waterflood.

These alternative methods are called enhanced oil recovery (EOR) methods. One such EOR method is the surfactant flood. Surfactants are effective in lowering the interfacial tension between oil and water to a level that promotes mobilization of trapped oil drops (see Shah and Schecter [24]). Surfactant floods (see Fathi and Ramirez [11]) have been used for EOR, and lessons learned from this have been applied for aquifer remediation (see Pope and Wade [21]). Another such method is polymer flooding. Polymer floods differ from waterfloods in that polymer floods rely on reducing mobility contrast between displacing and displaced fluids. Polymer flooding was attempted in the early 1970s. The idea of using polymer flooding to improve oil recovery started evolving through the 1970s and is well documented in various conference proceedings, books, and journal articles [9, 12, 15, 17, 20, 22, 24, 28]. In early 1980s, this polymer flooding process was mathematically formulated and solved numerically by Daripa et al. [5]. In most field tests with this flooding process, recovery was less than 10%. It was felt that this failure was perhaps due to (i) a loss of polymer in the rock matrix of porous media, (ii) polymer degradation, and (iii) a lack of understanding of some fundamental issues of this technology such as the timing of the start of this flood in relation to the waterflood that should precede this polymer flooding process. Before a systematic study could be undertaken to get to the bottom of all sources of this failure and thereby improve the polymer flooding strategy, interest in this polymer flooding process waned significantly in most countries, except in China, partly due to low labor cost. Corlay and Delamaide [1] present a whole history of

the Daqing polymer flooding project. The Daqing field is the largest oil field in the People's Republic of China, with original oil in place exceeding two billion tons.

Combining the above two methods into one that simultaneously reduces capillary pressure and reduces the mobility contrast is a better alternative perhaps. This alternative technology is called ASP (alkaline surfactant polymer) flooding and helps in addressing the challenges of recovering oil from subsea and deep-sea reservoirs and also from the formations where the mobility of the in-situ oil being recovered is significantly less than that of the drive fluid used to displace the oil. The alkaline in ASP is used so that it reacts with the acid components of crude oil and generates in-situ surfactant which overcomes the surfactant depletion in the liquid phases due to retention by the rock matrix. ASP flooding for EOR is relatively new and is being evaluated through laboratory investigations as well as field tests in many places. Successful results on ASP pilot tests in Cambridge [29], the Daqing and Gudong oil fields in China [8, 31], and many other oil fields around the globe, including those in Venezuela [30], have generated intense interest in ASP flooding [31]. The books by Littman [16] and Sorbie [26] and the articles by Needham and Doe [18], Zhijun and Yongmei [32], and Taylor and Nasr-El-Din [27] make the case, through all kinds of review, for ASP usage to improve oil recovery. Field tests are encouraging (recoveries are 25–30%), but at this recovery rate, economics are marginal at best. Investment in the basic research of this EOR method by ASP flooding (polymer flooding is a special case of ASP flooding) will ensure that this method has an important place in oil production for a long time to come.

Many of the modern EOR chemical flooding schemes use injection of a sequence of simple-to-complex fluids in succession with the hope of suppressing fingering instability and reducing capillary pressure, and thereby improving oil recovery. All these injection policies involve motion of an arbitrary number of sweeping interfaces. Unfortunately, even the basic stability results for flows involving motion of multiple interfaces, which can be helpful in the smart design of such flooding schemes, are not available. An attempt to address these challenges has been made in recent years by undertaking systematic linear stability studies of multilayer Hele-Shaw flows. Review of some of the key results known in this area will be presented in the next section. Careful reading of the next section is essential to recognize the significance of the universal results to be presented in section 4. Section 2 is then followed by section 3 on mathematical formulation. Sections 4 and 6 are about universal stability properties related to dispersion curves, unstable waves, and neutral waves of multilayer Hele-Shaw flows. Numerical results and the use of universal stability properties for the design of smart multilayer injection policies are presented in sections 5 and 7. These injection policies are based on two sets of parameters which have been derived in these sections. Finally, present conclusions in section 8.

2. Preliminaries. Two-layer Hele-Shaw flows in which a fluid is displacing another fluid of higher viscosity with both fluid layers extending up to infinity away from the common interface is the most celebrated case in the context of linear Saffman–Taylor instability of an interface separating two fluids. If μ_r is the viscosity of the displaced fluid, μ_l ($\mu_l < \mu_r$) is the viscosity of the displacing fluid, U is the constant velocity of the rectilinear flow, and the interfacial tension at the interface is constant T, then the growth rate σ_{st} of the interfacial disturbance having wavenumber k is given by

$$\sigma_{\rm st}(k) = \frac{Uk(\mu_r - \mu_l) - k^3 T}{\mu_r + \mu_l}, \tag{1}$$

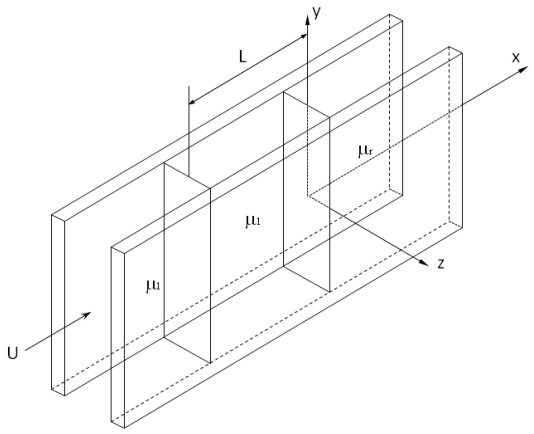

FIG. 1. *Three-layer fluid flow in a Hele-Shaw cell.*

from which it follows that the maximum growth rate $\sigma_{\rm sm}$ and corresponding dangerous wavenumber k_{sm} are given by

$$\sigma_{\rm sm} = \frac{2T}{(\mu_r+\mu_l)}\left(\frac{U(\mu_r-\mu_l)}{3T}\right)^{3/2}, \qquad k_{\rm sm} = \sqrt{\frac{U}{3T}(\mu_r-\mu_l)}. \tag{2}$$

The critical (also known as cut-off) wavenumber for which the wave is neutral (i.e., growth rate zero) is given by

$$k_{cr} = \sqrt{\frac{U}{T}(\mu_r-\mu_l)}. \tag{3}$$

The three-layer Hele-Shaw flow is an extension of this two-layer single-interface Hele-Shaw flow. The set-up is shown in Figure 1. The fluid upstream (i.e., as $x \to -\infty$) has a velocity $\mathbf{u} = (U, 0)$. The fluid in the extreme left layer with viscosity μ_l extends up to $x = -\infty$, the fluid in the extreme right layer with viscosity $\mu_r > \mu_l$ extends up to $x = \infty$, and the fluid in the middle layer with constant viscosity μ_1 ($\mu_r > \mu_1 > \mu_l$) is of finite extent of length L. Thus, this is a flow with two interfaces. Let T_0 and T_1 be the interfacial tensions of the leading and the trailing interfaces, respectively. Some facts about this problem from Daripa [4] will now be mentioned. There are two modes (eigenvalues) denoted by σ_+ and σ_- for each wave, and the corresponding dispersion relations $\sigma_+(k)$ and $\sigma_-(k)$ do not have explicit forms such as (1) in the two-layer case. However, these can be computed. Plots of these dispersion relations can be found in Daripa [4]. Exact formulas similar to (2) for the maximum growth rate and the most dangerous wavenumber are not available. However, an explicit formula for an upper bound on the maximum growth rate is given by (from Daripa [4])

$$\sigma < \sigma_{\rm u} = \max\left\{\frac{2T_0}{\mu_r}\left(\frac{U(\mu_r-\mu_1)}{3T_0}\right)^{3/2}, \frac{2T_1}{\mu_l}\left(\frac{U(\mu_1-\mu_l)}{3T_1}\right)^{3/2}\right\}, \tag{4}$$

and the cut-off wavenumbers k_1 and k_2 of $\sigma_+(k)$ and $\sigma_-(k)$, respectively, are given by

$$k_1 = \sqrt{\frac{U}{T_0}(\mu_r-\mu_1)} \quad \text{and} \quad k_2 = \sqrt{\frac{U}{T_1}(\mu_1-\mu_l)}. \tag{5}$$

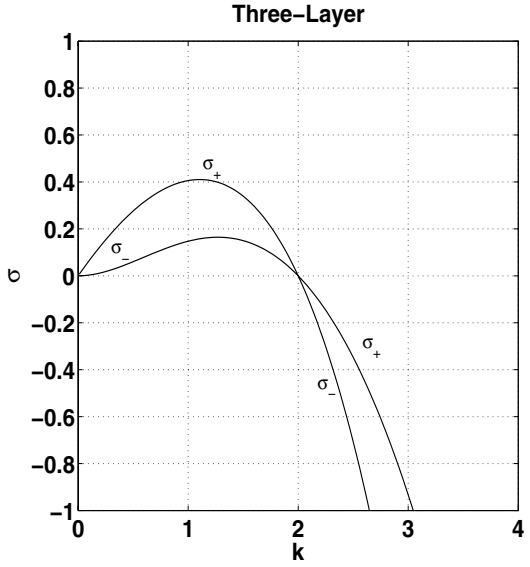

FIG. 2. *Plots of dispersion curves* $\sigma_-(k)$ *and* $\sigma_+(k) > \sigma_-(k)$ *for the three-layer case when* $\mu_1 = \mu_{\rm cr}$. *The parameter values used for these plots are* $\mu_l = 2, \mu_1 = 6, \mu_r = 10, T_0 = T_1 = U = 1$, *and* $L = 1$. *The viscosity* $\mu_1 = 6$ *is the critical viscosity* $\mu_{\rm cr}$ *given by formula* (6).

The necessary condition for a mode with wavenumber k to be unstable is $k \leq \max(k_1, k_2)$ and a sufficient condition is $k \leq \min(k_1, k_2)$. The two cut-off wavenumbers k_1 and k_2 become equal (called critical wavenumbers and denoted by $k_{\rm cr}$) when the middle layer viscosity μ_1 takes a specific value (called critical viscosity and denoted by $\mu_{\rm cr}$). These critical values are given by

$$\mu_{\rm cr} = \mu_r - \frac{T_0}{T_0 + T_1}(\mu_r - \mu_l), \qquad k_{\rm cr} = \sqrt{\frac{U}{T_0 + T_1}(\mu_r - \mu_l)}. \tag{6}$$

All waves in the range $0 < k < k_{\rm cr}$ are unstable when middle layer viscosity $\mu_1 = \mu_{\rm cr}$. The $k_{\rm cr}$ is the shortest unstable bandwidth $k_{\rm cr}$. In general, for other values of μ_1, the unstable bandwidth is $\max(k_1, k_2)$, where at least one of the modes is positive. Figure 2 shows the plots of the two dispersion curves when the middle layer viscosity $\mu_1 = \mu_{\rm cr}$ with the other parameter values $\mu_l = 2$, $\mu_r = 10$, $T_0 = T_1 = 1$, $U = 1$, and $L = 1$. We see that $\sigma_+ = \sigma_- = 0$ at $k = k_{\rm cr}$, as it should be.

In closing this section, there are several observations to be made for the three-layer case. It will be helpful in conclusion to see the generalization of these to the multilayer case and much more.

1. Notice the similarity between formula (2) for the maximum growth rate $\sigma_{\rm sm}$ in the two-layer case and formula (4) for the upper bound $\sigma_{\rm u}$ in the three-layer case. In the three-layer case, the strict upper bound $\sigma_{\rm u}$ is the maximum of the modified maximum individual Saffman–Taylor growth rates of two interfaces. This formula does not depend on L. However, the dispersion curves and the maximum growth rate depend on L (see Daripa [4]).
2. The cut-off wavenumbers k_1 and k_2 given by (5) are the same as the individual cut-off wavenumbers for the two interfaces that one obtains from applying

the pure Saffman–Taylor formula (3) to two individual interfaces with correct values of the viscosity across the interfaces used in this formula. An important thing to notice is that formulas (5) for k_1 and k_2 do not depend on the length L of the middle layer.

3. Notice that $\mu_{\rm cr}$ and $k_{\rm cr}$ given by (6) do not depend on the length L of the middle layer. Since the individual growth rates of the two interfaces are given by the Saffman–Taylor formulas in the limit $L \to \infty$, one can easily verify that the individual Saffman–Taylor growth rate of each of the two interfaces is zero at $k = k_{\rm cr}$ provided $\mu_1 = \mu_{\rm cr}$.
4. Notice the similarity between formula (3) for the critical (same as cut-off) wavenumber in the two-layer case and formula $(6)_2$ for the same wavenumber in the three-layer case. These two formulas, in fact, can be unified into one as

$$k_{\rm cr} = \sqrt{\frac{U}{T_{\rm total}}(\mu_r - \mu_l)}, \tag{7}$$

where $T_{\rm total}$ is the sum of interfacial tensions of all interfaces. For the pure Saffman–Taylor case, there is only one mode and hence only one cut-off wavenumber. In this case, the cut-off wavenumber is also called the critical wavenumber, though this is not the case in three-layer flows. In three-layer flows, there are two modes and thus two distinct cut-off wavenumbers k_1 and k_2 (see formula (5)) in general unless they become equal, $k_1 = k_2 = k_{\rm cr}$ when $\mu_1 = \mu_{\rm cr}$, which (see formula $(6)_1$), if written in terms of $T_{\rm total}$, becomes

$$\mu_{\rm cr} = \mu_r - \frac{T_0}{T_{\rm total}}(\mu_r - \mu_l). \tag{8}$$

5. In section 4, we will see that in the three-layer case there is another choice for the (critical) viscosity of the middle layer, namely $\sqrt{\mu_r\,\mu_l}$, when the unstable bandwidth will also be shortest as given by (7) provided the interfacial surface tensions are chosen carefully (special case of (34) with $N = 1$).

In this paper, we not only show the generalization of the above results to multi-layer Hele-Shaw flows but also discover new results even in the special case of three-layer flows. Results related to upper bounds on the maximum growth rate for the multi-layer Hele-Shaw flows are available from Daripa [3]. These results will be briefly mentioned in section 8. Next we briefly present the mathematical formulation and the numerical scheme to solve for the dispersion relations and obtain other analytical relations.

3. Mathematical formulation. The physical setup consists of rectilinear motion in a Hele-Shaw cell of many immiscible fluids having different viscosities. The physical setup for the special case when there are only three fluids is shown in Figure 1. This case is the building block for flows involving more than three fluids such as the one sketched in Figure 3 involving $N + 1$ number of interfaces with N number of interior layers.

The flow domain is $\Omega := (x, y) = \mathbb{R}^2$ (with a periodic extension of the setup in the y-direction). The fluid upstream (i.e., as $x \to -\infty$) has a velocity $\mathbf{u} = (U, 0)$ and constant viscosity μ_l which occupies the region $x < -L$ in the moving frame (moving with velocity $(U, 0)$). Similarly, the fluid in the region $x > 0$ in the moving frame has viscosity μ_r. There are N interior regions of equal length L/N in the interval $(-L, 0)$

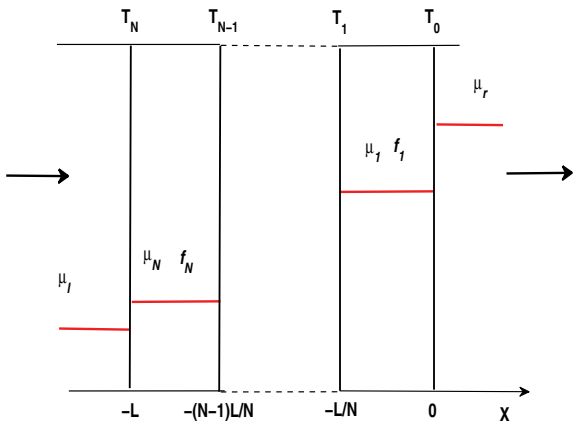

FIG. 3. *Multilayer fluid flow.*

(see Figure 3). These regions contain constant viscosity fluids μ_i, $i = 1, 2, \ldots, N$, such that viscosity increases in the direction of basic flow, i.e., $\mu_r > \mu_1 > \mu_2 > \mu_3 \ldots > \mu_N > \mu_l$. Thus, this set-up has $(N+1)$ interfaces located at $x = 0, -L/N, \ldots, -L$ with corresponding interfacial tension coefficients denoted by T_i, $i = 0, 1, \ldots, N$.

The fluid flow in each layer is described by the governing equations

$$\nabla \cdot \mathbf{u} = 0, \quad \nabla\, p = -\mu\, \mathbf{u}, \quad \frac{D\mu}{Dt} = 0, \tag{9}$$

where $\nabla = (\frac{\partial}{\partial x}, \frac{\partial}{\partial y})$ and $\frac{D}{Dt}$ is the material derivative. The first equation $(9)_1$ is the continuity equation for incompressible flow, the second equation $(9)_2$ is the Darcy's law (Darcy [2]), and the third equation $(9)_3$ is the advection equation for viscosity (Gorell and Homsy [13], Daripa and Pasa [7]). This last equation simply states that the viscosity is a property of the fluid and thus gets advected by the fluid. Below, we refer to this model as the Hele-Shaw model (see also Daripa [3], [4], Gorell and Homsy [13], and Pearson [19]).

The above system (9) admits a simple basic solution, namely, the whole fluid setup moves with velocity $(U, 0)$ with all its interfaces being planar, i.e., parallel to the y-axis. The pressure corresponding to this basic solution is obtained by integrating $(9)_2$. In a frame moving with velocity $(U, 0)$, the above system consisting of all planar interfaces and all fluid layers is stationary . Here and below, with slight abuse of notation, the same variable x is used in the moving reference frame. In linearized stability analysis by normal modes, disturbances (denoted by tilde variables below) in the moving reference frame are written in the form

$$(\widetilde{u}, \widetilde{v}, \widetilde{p}, \widetilde{\mu}) = (f(x), \psi(x), \phi(x), h(x))e^{(iky+\sigma t)} \tag{10}$$

where k is the wavenumber and σ is the growth rate. We then insert this disturbance form into the linearized disturbance equations obtained from (9) and also into the linearized dynamic and kinematic interfacial conditions. The details of these calculations when there is only one interior interface can be found in Daripa and Pasa [6]. Thus, we obtain the following system of N equations, one for each interior region:

$$f_{i_{xx}} - k^2 f_i = 0, \quad (i = 1, \ldots, N) \tag{11}$$

These equations also hold in the two exterior regions whose solutions due to exponential decay of eigenfunction in the far field are given by $f(x) = f(0)\exp(-kx),\ x > 0$, and $f(x) = f(-L)\exp(kx),\ x < -L$. Similarly, the interfacial conditions at $N+1$ interfaces are written down easily from extending single interface results (see Daripa and Pasa [6]) where we use the notation λ as the inverse of growth rate, i.e., $\lambda = 1/\sigma$:

$$-\mu_1 f_{1_x}^{-}(0) = (\mu_r k - \lambda E_0) f_1(0) \tag{12}$$

$$\mu_i f_{i_x}^{+}(-iL/N) - \mu_{i+1} f_{i+1_x}^{-}(-iL/N) = -\lambda E_i f_i(-iL/N), \quad i \in [1, N-1], \tag{13}$$

$$\mu_N f_{N_x}^{+}(-NL/N) = (\mu_l k - \lambda E_N) f_N(-NL/N), \tag{14}$$

Above we have used $\mu_0 = \mu_r$, $\mu_{N+1} = \mu_l$, and

$$E_i = k^2 U(\mu_i - \mu_{i+1}) - T_i k^4, \quad i = 0, 1, \ldots, N. \tag{15}$$

The continuity of eigenfunctions (i.e., $f_0(0) = f_1(0)$ and $f_N(-L) = f_{N+1}(-L)$) at the exterior interfaces have already been used in deriving (12) and (14) above. Similar conditions at $(N-1)$ interior interfaces give

$$f_i(-iL/N) = f_{i+1}(-iL/N) \ \ (i = 1, \ldots, N-1). \tag{16}$$

The general solution of (11) is $f_i(x) = C_i\ \exp(-kx) + D_i\ \exp(kx)$ for each interior domain $-iL/N < x < -(i-1)L/N$, $i = 1, 2, \ldots, N$. Substituting the solution into the boundary conditions (12)–(14) and (16) leads to a matrix equation $AX = 0$ for the unknown constant vector $X = (C_1, D_1, \ldots, C_N, D_N)$. The matrix A is a square matrix $(2N \times 2N)$ whose entries are denoted by A_{ij}, $i, j = 1, 2, \ldots, 2N$:

$$A = \begin{vmatrix} A_{11} & A_{12} & 0 & 0 & 0 & \cdots & 0 \\ A_{21} & A_{22} & A_{23} & A_{24} & 0 & \cdots & 0 \\ A_{31} & A_{32} & A_{33} & A_{34} & 0 & \cdots & 0 \\ & & & \cdots\cdots & & & \\ 0 & \cdots & 0 & A_{2N-2,2N-3} & A_{2N-2,2N-2} & A_{2N-2,2N-1} & A_{2N-2,2N} \\ 0 & \cdots & 0 & A_{2N-1,2N-3} & A_{2N-1,2N-2} & A_{2N-1,2N-1} & A_{2N-1,2N} \\ 0 & \cdots & 0 & 0 & 0 & A_{2N,2N-1} & A_{2N,2N} \end{vmatrix}.$$

As an example for the case of three intermediate layers A_{ij} we give

$$\begin{aligned}
&A_{11} = \sigma(\mu_1 - \mu_r)k + E_0, \ \ A_{12} = -\sigma(\mu_1 + \mu_r)k + E_0, \\
&A_{21} = (-\sigma\mu_1 k + E_1)e^{(kL/N)}, A_{22} = (\sigma\mu_1 k + E_1)e^{(-kL/N)}, \\
&A_{23} = \sigma\mu_2 k e^{(kL/N)}, A_{24} = \sigma\mu_2 k e^{(kL/N)}, \\
&A_{31} = -e^{(kL/N)}, A_{32} = e^{(-kL/N)}, A_{33} = e^{(kL/N)}, A_{34} = -e^{(-kL/N)}, \\
&A_{43} = (-\sigma\mu_2 k + E_2)e^{(2kL/N)}, A_{44} = (\sigma\mu_2 k + E_2)e^{(-2kL/N)}, \\
&A_{45} = \sigma\mu_3 k e^{(2kL/N)}, A_{46} = -\sigma\mu_3 k e^{(-2kL/N)}, \\
&A_{53} = -e^{(2kL/N)}, A_{54} = e^{(-2kL/N)}, A_{55} = e^{(2kL/N)}, A_{56} = -e^{(-2kL/N)}, \\
&A_{65} = (\sigma(\mu_4 + \mu_l)k - E_3)e^{(3kL/N)}, A_{66} = (\sigma(-\mu_4 + \mu_l)k - E_3)e^{(-3kL/N)}.
\end{aligned}$$

The first line of matrix A comes from the boundary condition in (12), the second and fourth lines are from the boundary condition in (13), the third and fifth lines are from the boundary condition in (16), and the last line is from the boundary condition in (14). We notice that in this example, there are no σ terms in the third and fifth lines. We then conclude that there are no σ in $(N-1)$ rows of $(2N \times 2N)$ matrix A. The solvability condition, namely, the determinant of matrix $\det(A) = 0$ for a nontrivial solution, leads to the dispersion relation. Since the highest degree of $\det(A) = 0$ is $(N+1)$, there will be $(N+1)$ roots corresponding to $(N+1)$ interfaces. These roots are found numerically to obtain the dispersion relations. These numerically obtained dispersion relations will be plotted in the sections below as necessary.

4. Universal stability properties. The dispersion curves $\{\sigma_i(k),\, i = 0, \ldots, N\}$ are computed for some choices of N by solving the $(N+1)$ degree polynomial resulting from the solvability condition $\det(A) = 0$. These curves are shown later. First we derive some exact results from analyzing this solvability condition. We notice from the form of the matrix A and its entries in the previous section that if $E_i = 0$ for any one of $i = 0, 1, \ldots, N$, then $\det(A)$ will be of the following form:

$$\det(A) = \sigma(k)a(\sigma(k)), \tag{17}$$

where $a(\sigma(k))$ is a function of σ and k. Since $E_i = k^2U(\mu_i - \mu_{i+1}) - T_ik^4 = 0$ at $k = k_i \equiv \sqrt{U(\mu_i - \mu_{i+1})/T_i}$, it follows from the solvability condition $\det(A) = 0$ and (17) that there is one mode $\sigma_i(k) = 0$ at $k = k_i$. In general, each of the modes $\sigma_i(k) = 0$ at a wavenumber k_i is distinct from the others, and thus we have

$$k_i = \sqrt{\frac{U(\mu_i - \mu_{i+1})}{T_i}}, \quad i = 0, 1, \ldots, N. \tag{18}$$

These are the cut-off wavenumbers for the $(N+1)$ dispersion curves. Notice that these cut-off wavenumbers do not depend on L and thus, not surprisingly, correspond to cut-off wavenumbers for dispersion curves of $N+1$ individual interfaces determined simply by applying the pure Saffman–Taylor formula (3) to all these individual interfaces with correct values of the viscosity across the interfaces used in this formula. If we define

$$k_{\max} = \max(k_0, k_1, \ldots, k_N) \quad \text{and} \quad k_{\min} = \min(k_0, k_1, \ldots, k_N), \tag{19}$$

then it is obvious that at least one of the modes is positive if wavenumber k satisfies

$$k \le k_{\max}, \tag{20}$$

and all modes are positive for a wave satisfying

$$k \le k_{\min}. \tag{21}$$

Thus inequality (20) is a necessary condition for instability of a mode with wavenumber k, whereas inequality (21) is a sufficient condition for instability of a mode with wavenumber k. Notice that $k_{\max}$ and $k_{\min}$ are both L-independent.

Moreover, when $E_0 = \cdots = E_N = 0$ at the wavenumber $k = k_{cr}$, that means $k_0 = \cdots = k_N = k_{cr}$. In this case, the determinant of matrix A has the following form (see the matrix A and its entries in the previous section):

$$\det(A) = b(k_{cr})\sigma^{N+1}, \tag{22}$$

where $b(k_{cr})$ is a function of k_{cr}. It is easy to see that the $(N+1)$ roots of (22) are all zero, that is,

$$\sigma_i = 0, \qquad i = 0, 1, \ldots, N. \tag{23}$$

We can solve for k_{cr} and the "critical" viscosities $\mu_{cr}^{(i)}, i = 1, \ldots, N$ for the N layers from $(N+1)$ equations $E_i = 0,\ i = 0, 1, \ldots, N$, or, equivalently, from

$$\left.\begin{array}{l} k_{cr}^2 U(\mu_r - \mu_1) - T_0 k_{cr}^4 = 0, \\ k_{cr}^2 U(\mu_1 - \mu_2) - T_1 k_{cr}^4 = 0, \\ \cdots\cdots \\ k_{cr}^2 U(\mu_N - \mu_l) - T_N k_{cr}^4 = 0. \end{array}\right\} \tag{24}$$

By adding all the above equations together, below we solve for k_{cr} in terms of viscosities of extreme layers. Then substituting the formula of k_{cr} in each of the above equations, we obtain the following formulas for the N critical viscosities $\mu_{cr}^{(1)}, \ldots, \mu_{cr}^{(N)}$.

$$\left.\begin{array}{l} k_{cr} = \sqrt{\frac{U(\mu_r - \mu_l)}{T_{\text{total}}}}, \\ \mu_{cr}^{(1)} = \mu_r - \frac{T_0}{T_{\text{total}}}(\mu_r - \mu_l), \\ \mu_{cr}^{(2)} = \mu_{cr}^{(1)} - \frac{T_1}{T_{\text{total}}}(\mu_r - \mu_l), \\ \cdots\cdots \\ \mu_{cr}^{(N-1)} = \mu_{cr}^{(N-2)} - \frac{T_{N-2}}{T_{\text{total}}}(\mu_r - \mu_l), \\ \mu_{cr}^{(N)} = \mu_{cr}^{(N-1)} - \frac{T_{N-1}}{T_{\text{total}}}(\mu_r - \mu_l), \end{array}\right\} \tag{25}$$

where $T_{\text{total}} = (T_0 + T_1 + \cdots + T_N)$ is the sum of interfacial tensions of all $(N+1)$ interfaces. It is easy to verify that all the above results when $N = 1$ are in agreement with the results for the three-layer case given in section 2.

In general, all waves satisfying $k < k_{\max}$ (see $(19)_1$) are unstable since at least one of the modes is always positive in this range. However, when fluids in N layers have critical viscosities μ_{cr} according to the formulas given above, the unstable bandwidth is given by k_{cr}. We claim that this is the shortest bandwidth for unstable waves meaning $k_{cr} \le k_{\max}$, similar to the three-layer case. We show this next. We recall the following inequality

$$\frac{\sum_{i=1}^n P_i}{\sum_{i=1}^n Q_i} \le \max_i \frac{P_i}{Q_i}, \tag{26}$$

which holds for arbitrary n under the condition $P_i > 0$, $Q_i > 0$ $(i = 1, \ldots, n)$. Using this inequality with $P_i = U(\mu_i - \mu_{i+1}), Q_i = T_i$, we obtain

$$\frac{U(\mu_r - \mu_1) + U(\mu_1 - \mu_2) + \cdots + U(\mu_{N+1} - \mu_l)}{T_0 + T_2 + \cdots + T_N} \le \max_i \frac{U(\mu_i - \mu_{i+1})}{T_i} \tag{27}$$

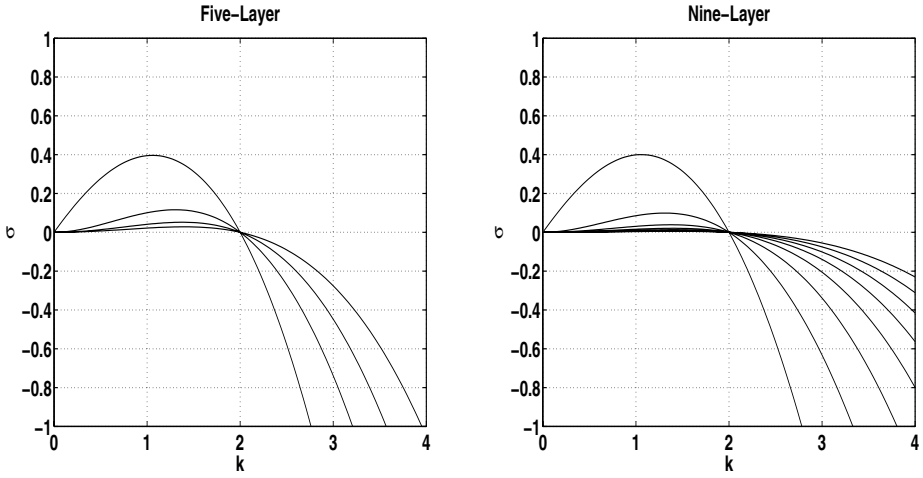

FIG. 4. *Dispersion relations: growth rates versus wavenumber k. Five-layer parameter values are viscosity $\mu = (2, 4, 6, 8, 10)$, $N = 3$, $T_0 = \cdots = T_3 = 1/2$, $U = 1$, and $L = 1$. Nine-layer parameter values are viscosity $\mu = (2, 3, 4, 5, 6, 7, 8, 9, 10)$, $N = 7$, $T_0 = \cdots = T_7 = 1/4$, $U = 1$, and $L = 1$.*

or, equivalently,

$$\frac{U(\mu_r - \mu_l)}{T_{\text{total}}} \leq k_{\max}^2, \tag{28}$$

where we have used the definition $(19)_1$ for $k_{\max}$. Since the left side of inequality (28) is k_{cr}^2, it follows that $k_{cr} \leq k_{\max}$, a generalization of the same result from the three-layer case.

5. Numerical results. It is interesting to observe that the shortest bandwidth k_{cr} is dependent only on U, $(\mu_r - \mu_l)$, and T_{total}. This means that the critical wave number k_{cr} will remain the same for an arbitrary number of internal layers, N, provided U, $(\mu_r - \mu_l)$, and T_{total} are kept fixed regardless of individual nonzero interfacial tension values of $N + 1$ interfaces and the internal N layers' fluid viscosities are $\mu_{cr}^{(i)}, i = 1, \ldots, N$ given by (25). Figure 4 shows the dispersion plots for five-layer and nine-layer Hele-Shaw flows, respectively, with the same value for U, the same total interfacial tension T_{total}, and the same viscosity difference $(\mu_r - \mu_l)$ between two extreme-layer fluids. Notice that all modes have value zero at $k = k_{cr}$, as it should be.

The pure Saffman–Taylor case is a special case of the multilayer case when $N = 0$ corresponding to no internal layer (layer of finite thickness). From an EOR perspective, one of the reasons for having several layers with the constant viscosity of each layer increasing in the direction of basic velocity U is obviously to stabilize the system, i.e., to have $\sigma_{\max}$ of the multilayer system lower than the pure Saffman–Taylor growth rate σ_{sm}. Notice that we used the words "stabilize the system" here and below to mean "to make the system less unstable." In Daripa [3], a family of upper bounds for the maximum growth rate for the multilayer system has been presented, one of which is the extension of formulas (4) from three-layer to multilayer. In general, in the multilayer case with appropriate choices of interfacial tensions and the intermediate

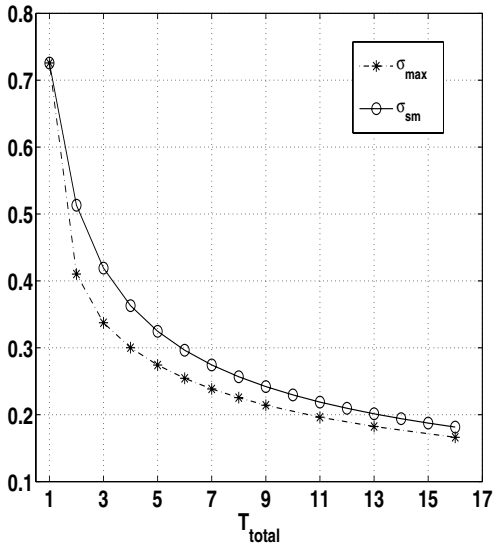

FIG. 5. *The maximum growth rate $\sigma_{\max}$ for multilayer flows with group-1 parameters and the maximum growth rate for Saffman–Taylor σ_{sm} versus the interfacial tension T. The parameter values are $\mu_l = 2$, $\mu_r = 10$, $T_i = 1$ $(i = 0, \ldots, N)$, $U = 1$, and $L = 1$.*

layer fluids' constant viscosities, one can get significant improvement in stability over the pure Saffman–Taylor case. But using the new results given above, we can now a priori decide on various parameter values to home in on not only a more stabilized system but also a shortest unstable band $k_{\rm cr}$. This is what we show next.

As we have seen above, for the shortest unstable bandwidth k_{cr} one can calculate $\mu_{cr}^{(i)}, i = 1, \ldots, N$ from μ_r, μ_l, and $T_{\rm total}$ regardless of the number of interfaces and their interfacial tensions $T_i, i = 0, \ldots, N$, so long as these add up to $T_{\rm total}$. But how does one select $T_i, i = 1, \ldots, N$, and L to design the most stable (least unstable) multilayer system? Consider the simplest case when all interfacial tensions are the same, say $T_0 = T_1 = \cdots = T_N$ for a given $T_{\rm total}$ from which all $\mu_{cr}^{(i)}, i = 1, \ldots, N$ are computed using formulas (25) for the multilayer system. We call this set of values for parameters $\{\mu_{cr}^{(i)}, T_i, i = 1, \ldots, N\}$ group-1. Figure 5 shows plots of the maximum growth rate $\sigma_{\max}$ for the multilayer system and the maximum pure Saffman–Taylor growth rate σ_{sm} against $T_{\rm total}$. For a given $T_{\rm total}$, the value of σ_{sm} is computed using the formula $(2)_1$. It is clear that $\sigma_{\max}$ and σ_{sm} both decrease with increasing T. The general trend shows that $\sigma_{\max}$ is smaller than σ_{sm} for a fixed total interfacial tension $T_{\rm total}$. But with increasing T, the difference between $\sigma_{\max}$ and σ_{sm} becomes smaller. Nonetheless, we see that the multilayer Hele-Shaw flows with group-1 values of the parameters used above are less unstable than the corresponding pure Saffman–Taylor case.

According to formulas (25), individual interfacial tension values for given μ_r and μ_l determine the values of $\{\mu_{cr}^{(i)}, i = 1, \ldots, N\}$. Therefore, the choice of these interfacial tension values is crucial for stabilization under the constraint that $T_{\rm total}$ remains the same regardless of the number of interfaces so that all these flows have the same shortest unstable bandwidth $k_{\rm cr}$ (see formulas (25)). Although the multilayer Hele-Shaw flows with group-1 values of the parameters used above are less unstable than

the corresponding pure Saffman–Taylor case, it follows from formulas (25) that there exist infinitely many sets of values for $\{T_i, i = 1, \ldots, N\}$ for the same given T_{total} $(= N + 1$ for the example above) because this total interfacial tension can be unevenly distributed in infinite ways among $N + 1$ interfaces. Equidistribution of T_{total} among $N + 1$ interfaces as in the previous example may not be the best for stabilization. There may be other, better choices of $\{T_i, i = 1, \ldots, N\}$ for the same given T_{total}.

6. Universality continued. Below, using intuition and heuristic reasoning we show another way to choose the set $\{T_i, i = 1, \ldots, N\}$ for some given T_{total} that has no influence on the choice of $\{\mu_{cr}^{(i)}, i = 1, \ldots, N\}$, unlike the previous case (see formulas (25)), and results in a more stable system with shortest unstable bandwidth k_{cr}. We know that when $L \to \infty$, individual interfacial instabilities should be independent of each other. Therefore, all $(N + 1)$ dispersion curves $\sigma_i(k)$, $i = 0, \ldots, N$, for the multilayer system should approach $(N+1)$ pure Saffman–Taylor dispersion curves, one corresponding to each individual interface, when $L \to \infty$. In this limit, the maximum growth rate $\sigma_{\max} = \max_i\{\max_k \sigma_i(k)\}$ of the multilayer system can be described by the pure Saffman–Taylor problem, which is

$$\sigma_{\text{sm,max}} = \max_i\{\sigma_{sm}^{(i)}\}, \tag{29}$$

where $\sigma_{sm}^{(i)} = \max_k \sigma_{st}^{(i)}(k)$ is the maximum Saffman–Taylor growth rate of the ith interface. The problem is to find an optimal group of $\mu_{cr}^{(i)}$ and T_i that minimizes the maximum growth rate $\sigma_{\max}$ of the multilayer system. However, this minimization problem is approximately equivalent to minimizing the $\sigma_{\text{sm,max}}$ defined above by (29) because the maximum growth rate of the multilayer system decreases exponentially with L (see Daripa [4]). Therefore, the problem now is to find the values of $\{\mu_{cr}^{(i)}, i = 1, \ldots, N\}$ and $\{T_i, i = 1, \ldots, N + 1\}$ that will minimize the maximum of $\{\sigma_{sm}^{(i)}, i = 1, \ldots, N+1\}$. The solution of this problem becomes easier if all $\{\sigma_{sm}^{(i)}, i = 1, \ldots, N+1\}$ are taken equal. Even though this heuristic reasoning is not exactly a proof, we will see later that results obtained from this hypothesis provide a remarkable gain in stabilization compared to group-1. In fact, we can do better than this. We can find $\mu_{cr}^{(i)}$ and T_i such that all individual interfacial dispersion curves $\sigma_{\text{st}}^{(i)}(k)$, $i = 1, \ldots, N$ are identical. Then naturally all $\{\sigma_{sm}^{(i)}, i = 1, \ldots, N + 1\}$ will be equal. Thus, next we select $\mu_{cr}^{(i)}$, $i = 1, \ldots, N$, and T_i, $i = 1, \ldots, N$, that satisfy the following equations so that all $\sigma_{\text{st}}^{(i)}(k)$, $i = 1, \ldots, N$, are equal (see formula (1) for $\sigma_{\text{st}}(k)$):

$$\frac{Uk(\mu_r - \mu_1)}{\mu_r + \mu_1} = \frac{Uk(\mu_1 - \mu_2)}{\mu_1 + \mu_2} = \cdots = \frac{Uk(\mu_N - \mu_l)}{\mu_N + \mu_l} \tag{30}$$

and

$$\frac{T_0 k^3}{\mu_r + \mu_1} = \frac{T_1 k^3}{\mu_1 + \mu_2} = \cdots = \frac{T_N k^3}{\mu_N + \mu_l}, \tag{31}$$

so that

$$\sigma_{st}^{(0)}(k) = \sigma_{st}^{(1)}(k) = \cdots = \sigma_{st}^{(N)}(k) \tag{32}$$

for all k. Therefore, zeros k_i of all dispersion curves $\sigma_{st}^{(i)}, i = 0, \ldots, N$, are equal to each other, i.e.,

$$k_0 = \cdots = k_N = \sqrt{\frac{U}{T_{\text{total}}}(\mu_r - \mu_l)} \equiv k_{cr}. \tag{33}$$

By solving for $\mu_{cr}^{(i)}$ and T_i from (30) and (31), we get a new group of viscosities and interfacial tensions for the shortest width of the unstable band. We call this group-2 parameters:

$$\left.\begin{aligned}
&\mu_{cr}^{(1)} = \mu_r^{\frac{N}{N+1}} \mu_l^{\frac{1}{N+1}}, \\
&\mu_{cr}^{(2)} = \mu_r^{\frac{N-1}{N+1}} \mu_l^{\frac{2}{N+1}}, \\
&\cdots\cdots \\
&\mu_{cr}^{(N)} = \mu_r^{\frac{1}{N+1}} \mu_l^{\frac{N}{N+1}}, \\
&T_0 = \frac{(\mu_r + \mu_{cr}^{(1)})}{\mu_r + \mu_l + 2(\mu_{cr}^{(1)} + \cdots + \mu_{cr}^{(N)})} T_{\text{total}}, \\
&T_1 = \frac{(\mu_1 + \mu_{cr}^{(2)})}{\mu_r + \mu_l + 2(\mu_{cr}^{(1)} + \cdots + \mu_{cr}^{(N)})} T_{\text{total}}, \\
&\cdots\cdots \\
&T_N = \frac{(\mu_{cr}^{(N)} + \mu_l)}{\mu_r + \mu_l + 2(\mu_{cr}^{(1)} + \cdots + \mu_{cr}^{(N)})} T_{\text{total}},
\end{aligned}\right\} \tag{34}$$

where $T_{\text{total}} = (T_0 + T_1 + \cdots + T_N)$. Note that notations for the viscosities of all internal layer fluids computed with group-1 formulas (25) are the same as those computed with group-2 formulas (34). However, this should not cause any problem below as these are always referred to by their respective groups. Notice that in the three-layer case ($N = 1$), the above formulas yield the group-2 critical viscosity of the fluid in the middle layer as $\mu_{cr}^{(1)} = \sqrt{\mu_r \mu_l}$ and the interfacial tensions $T_0 = \sqrt{\frac{\mu_r}{\mu_r+\mu_l}}\, T_{\text{total}}$ and $T_1 = \sqrt{\frac{\mu_l}{\mu_r+\mu_l}}\, T_{\text{total}}$. It is easy to verify that the cut-off wavenumbers k_1 and k_2 of both modes in this case are k_{cr} given by (33). It is interesting to notice from the formulas above that the viscosities of the fluid layers in succession from left to right in the direction of displacement form a geometric series with geometric ratio $(\mu_r/\mu_l)^{1/(N+1)}$.

7. Numerical results continued. For given values of T_{total}, μ_r, and μ_l, values of the group-2 parameters $\mu_{cr}^{(i)}$ and T_i are calculated using the above formulas (34). Using these interfacial tensions $T_i, i = 0, \ldots, N$, viscosities $\mu_{cr}^{(i)}, i = 1, \ldots, N$, of the interior layer fluids, and given values of U and L, eigenvalues $\sigma^{(i)}(k)$ are numerically computed (see section 3). Figures 6 and 7 show the plots of dispersion curves $\sigma^{(i)}(k)$ versus wavenumber k for three-, four- and five-layer Hele-Shaw flows when $L = 1$ and $L = 5$, respectively, with $T_{\text{total}} = 2, U = 1$, $\mu_r = 10$, and $\mu_l = 2$ fixed. It is clear that when L increases, all dispersion curves for the multilayer system come closer to each other. Furthermore, the shortest bandwidth k_{cr} is equal to 2 as predicted by (33).

In what follows, we compare the effect of the two groups of parameters for $\mu_{cr}^{(i)}$ and T_i, one computed from (25) and the other from (34). Figure 8 shows plots of $\sigma_{\max}$ versus L in three-, four-, and five-layer Hele-Shaw flows for both groups of parameters.

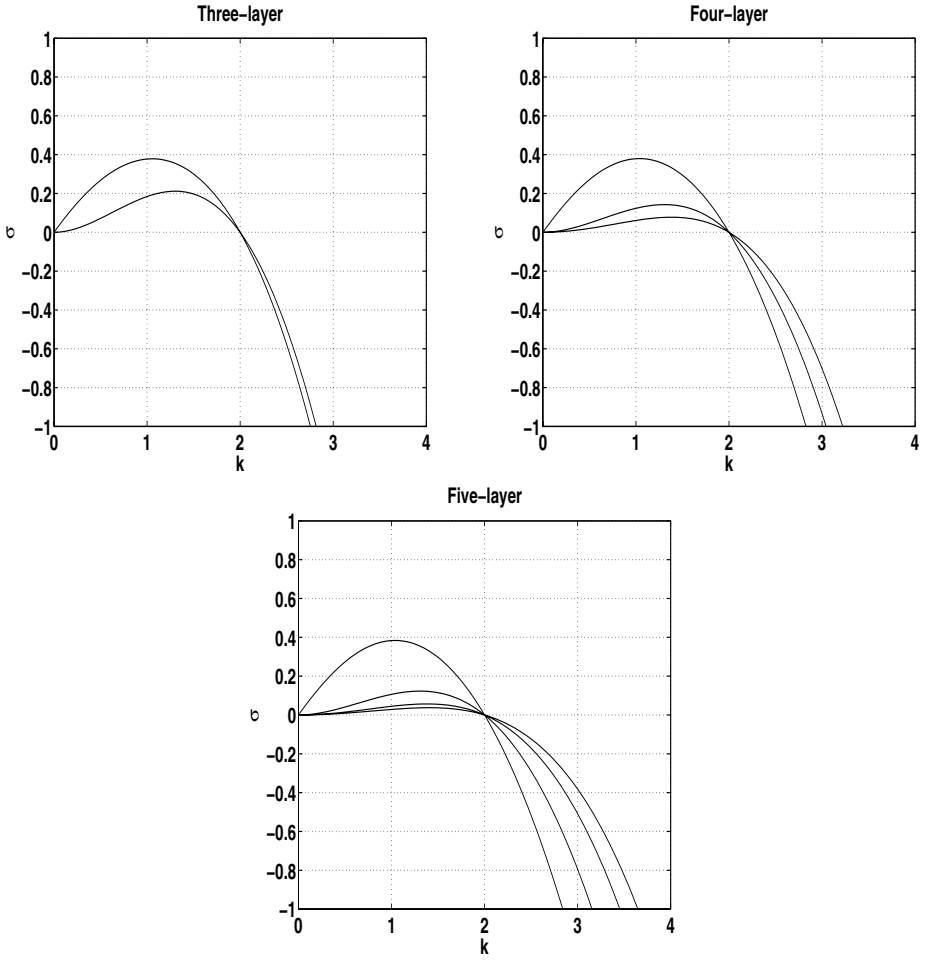

FIG. 6. *Dispersion curves for* (25) *when* $L = 1$*: Growth rates* σ *versus wavenumber* k *for three-, four-, and five-layer cases. Parameter values are as follows:* $\mu = (2, 4.472, 10)$*,* $T = (1.382, 0.618)$ *in the three-layer case;* $\mu = (2, 3.42, 5.848, 10)$*,* $T = (1.038, 0.607, 0.355)$ *in the four-layer case;* $\mu = (2, 2.9907, 4.472, 6.6874, 10)$*,* $T = (0.8281, 0.5538, 0.3704, 0.2477)$ *in the five-layer case. In all cases,* $U = 1$ *and* $T_{\text{total}} = 2$*.*

Plots in both panels show that flow becomes more stable with increasing number of layers, with all other parameter values fixed. We see, as expected, that the effect of L quickly saturates with both groups of parameters. Notice the significantly improved stabilization capacity of the set of values corresponding to group-2 parameters (Figure 8, right panel) compared to that for the set of group-1 parameters used for plots in the left panel. Toward this end, we mention that for given T_{total}, μ_r, and μ_l, there is only one set of values for group-2 parameters as opposed to infinitely many set of values for group-1 parameters because of free variables T_i subject to the condition that all these interfacial tensions must add up to given T_{total}. Some of these sets of values from group-1 can even make the system more unstable, but many of these sets will also stabilize the system. The choice of the set used for the plots in the left panel of Figure 8 is a typical case. Many experiments with various other choices of the set from this group-1 with T_{total}, μ_r, and μ_l fixed at the values mentioned in the caption

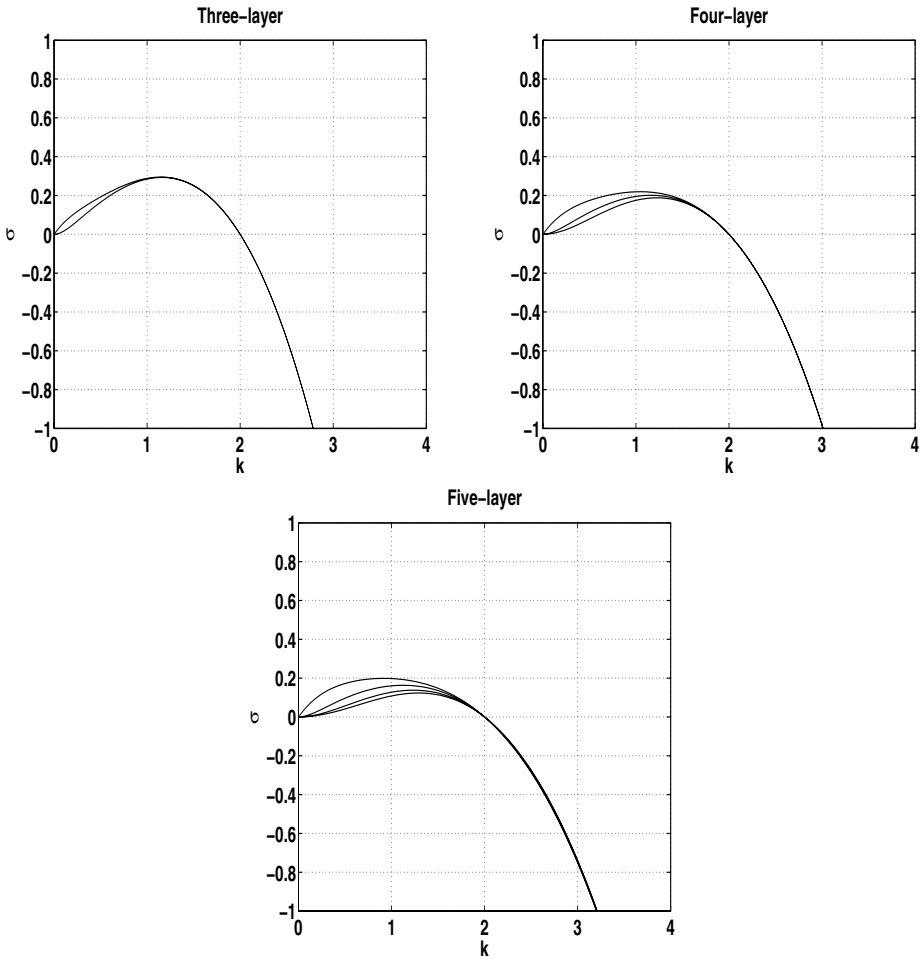

FIG. 7. *Dispersion curves for* (25) *when* $L = 5$*: Growth rates* σ *versus wavenumber* k *for three-, four-, and five-layer cases. Parameter values are as follows:* $\mu = (2, 4.472, 10)$*,* $T = (1.382, 0.618)$ *in the three-layer case;* $\mu = (2, 3.42, 5.848, 10)$*,* $T = (1.038, 0.607, 0.355)$ *in the four-layer case;* $\mu = (2, 2.9907, 4.472, 6.6874, 10)$*,* $T = (0.8281, 0.5538, 0.3704, 0.2477)$ *in the five-layer case. In all cases,* $U = 1$ *and* $T_{\text{total}} = 2$*.*

to Figure 8 show that their stabilization capacities do not exceed that shown in the right panel of Figure 8 with group-2 parameters' values.

In closing this section, we mention that we have shown the universality of the formulas such as (5) and (6) for k_i, critical viscosity, and critical wavenumber. In fact, we have discovered another group (34) of critical viscosities for the same critical wavenumber $(6)_2$. It is worth pointing out that the formula such as (2) for the maximum growth rate and the most dangerous wavenumber for the pure Saffman–Taylor case have no universality appeal for the multilayer case. The only universality related to the growth rate is a generic pattern of the formula for the upper bound which can be found in Daripa [3] (see formulas (99), (103), and (105) there). In the special case of three layers ($N = 1$), these formulas for the upper bound reduce to (4).

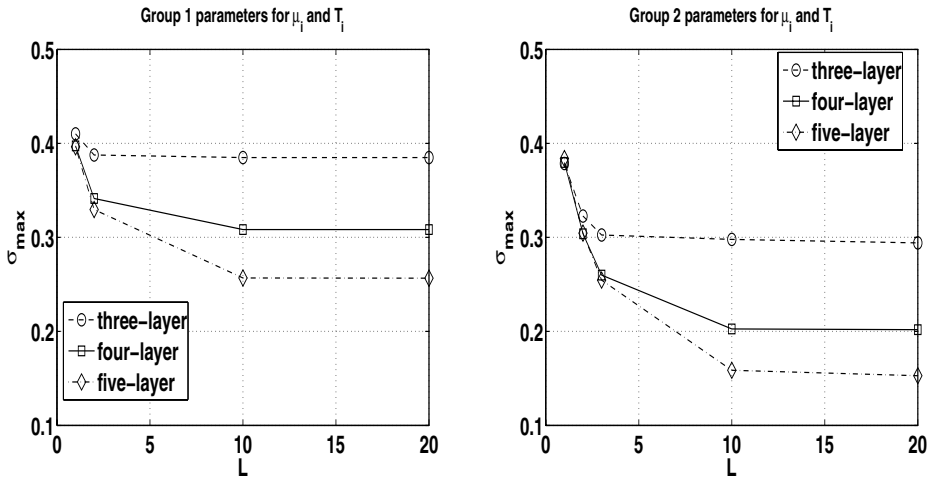

FIG. 8. *Comparison of stabilization capacity of two groups* (25) *and* (34) *for the same* T_{total}, U, *and* L: *Plots of the maximal growth rate for* $\sigma_{\max}$ *versus* L *for three-, four-, and five-layer cases. The parameters for the left plot are as follows:* $\mu = (2, 6, 10)$, $T_0 = T_1 = 1$ *in the three-layer case;* $\mu = (2, 4.67, 7.34, 10)$, $T_0 = T_1 = T_2 = 2/3$ *in the four-layer case;* $\mu = (2, 4, 6, 8, 10)$, $T_0 = T_1 = T_2 = T_3 = 1/2$ *in the five-layer case. For the right plot:* $\mu = (2, 4.472, 10)$, $T = (1.382, 0.618)$ *in the three-layer case;* $\mu = (2, 3.42, 5.848, 10)$, $T = (1.038, 0.607, 0.355)$ *in the four-layer case;* $\mu = (2, 2.9907, 4.472, 6.6874, 10)$, $T = (0.8281, 0.5538, 0.3704, 0.2477)$ *in the five-layer case. In all cases:* $U = 1$ *and* $T_{\text{total}} = 2$.

8. Conclusions. In this paper, we have obtained linear stability results that are universal for multilayer Hele-Shaw flows in the sense that the results hold for flows involving an arbitrary number of interfaces. To summarize, we list the universal stability results below:

1. The cut-off wavenumbers k_i, $i = 0, 1, \ldots, N$ given by (18) are universal, meaning that they hold for flows with any number of interfaces. Notice two important facts about this: (i) cut-off wavenumbers are pure Saffman–Taylor cut-off wavenumbers for individual interfaces; (ii) these cut-off wavenumbers do not depend on the length, L, of the middle layer. These properties are universal as well.
2. The unstable bandwidth $k_{\max}$ given by $(19)_1$ is universal as well and does not depend on L. The shorter bandwidth $k_{\min}$ given by $(19)_2$ which contains unstable waves having both modes (σ_+, σ_-) positive is also universal. These bandwidths also do not depend on L.
3. The critical values $\mu_{\text{cr}}^{(i)}$ and k_{cr} given by formulas (25) for group-1 and by formulas (34) for group-2 are universal as well and do not depend on L. Since individual growth rates of all interfaces are given by the Saffman–Taylor formulas in the limit $L \to \infty$, one can easily verify that individual Saffman–Taylor growth rates of all interfaces are zero at $k = k_{\text{cr}}$ provided viscosities of the fluids in the N interior layers are $\mu_{\text{cr}}^{(i)}, i = 1, \ldots, N$ (either from group-1 or group-2), and in the case of group-2, the interfacial tensions are T_i given by (34).

Even though the above stability results do not depend on L, it is important to emphasize that some stability results depend on L and have been addressed in Daripa [4]. For example, dispersion curves and the maximum growth rate depend on L. This is

expected, as stability of individual interfaces is coupled nonlinearly as reflected in the expression of matrix A (see section 3). This system decouples into individual interface problems only in the limit of $L \to \infty$. The universal stability results derived above are special considering the fact that the problem is nonlinear and does not decouple into individual problems for finite values of L, even though it appears that way from some of the universality results obtained in this paper. The above universality results should be useful for stabilization and understanding of flow features in unstable multilayer Hele-Shaw flows. Application of these new results to stabilization of multilayer Hele-Shaw flows has been demonstrated in this paper.

In closing, we briefly discuss the relevance of our results to chemical EOR. One can set up the initial data and the parameter values (such as viscosities and interfacial tensions) in a reservoir simulator corresponding to any specific flooding strategy desired, including the ones based on results obtained in this paper. Then various quantities of interest such as oil recovered, fractional area swept, etc., resulting from any specific flooding strategy can be computed using the simulator. This process will allow evaluation of relative performance of various flooding strategies and test the merit of our results. However, a few points are worth mentioning since the results of this paper are based on the Hele-Shaw model, whereas most reservoir simulators are based on the Buckley–Leverett model. It has been argued in Daripa [4] and in the first paragraph of section 1 that both of these models will lead to similar results for homogeneous reservoirs. Our results may be also relevant for heterogeneous reservoirs. Research into these topics falls outside the scope of this paper.

Acknowledgments. It is a pleasure to thank the two reviewers for helpful suggestions. X.D. would like to acknowledge the postdoctoral support from the Qatar Foundation. The statements made herein are solely the responsibility of the authors.

REFERENCES

[1] Ph. Corlay and E. Delamaide, *Evaluation and future of polymer injection in the Daqing field*, Revue de l'institut Français du Pétrole, 50 (1995), pp. 237–247.
[2] H. Darcy, *Les fontaines publiques de la ville de Dijon*, Libraire des Corps Impériaux des Ponts et Chaussées et des Mines, Paris, 1856.
[3] P. Daripa, *Hydrodynamic stability of multi-layer Hele-Shaw flows*, J. Stat. Mech. Theory Exp., 2008, no. 12, P12005.
[4] P. Daripa, *Studies on stability in three-layer Hele-Shaw flows*, Phys. Fluids. 20 (2008), 112101.
[5] P. Daripa, J. Glimm, B. Lindquist, and O. McBryan, *Polymer floods: A case study of nonlinear wave analysis and of instability control in tertiary oil recovery*, SIAM J. Appl. Math., 48 (1988), pp. 353–373.
[6] P. Daripa and G. Pasa, *New bounds for stabilizing Hele-Shaw flows*, Appl. Math. Lett., 18 (2005), pp. 1293–1303.
[7] P. Daripa and G. Pasa, *On the growth rate for three-layer Hele-Shaw flows: Variable and constant viscosity cases*, Internat. J. Engrg. Sci., 43 (2005), pp. 877–884.
[8] W. Demin, C. Jiecheng, W. Junzheng, Y. Zhenyu, and L. Hongfu, *Summary of ASP pilots in Daqing oil field*, in Proceedings of the SPE Asia Pacific Improved Oil Recovery Conference, Society of Petroleum Engineers, Allen, TX, 1999, 57288-MS.
[9] T. Doscher and F. Wise, *Enhanced crude-oil recovery potential: Estimate*, J. Petroleum Technology, 28 (1976), pp. 575–585.
[10] P. G. Drazin and W. H. Reid, *Hydrodynamic Stability*, Cambridge University Press, Cambridge, UK, 1981.
[11] Z. J. Fathi and W. Ramirez, *Optimal injection policies for enhanced oil recovery: Part 2—surfactant flooding*, SPE J., 24 (1984), 12814-PA.
[12] F. Fayers, ed., *Enhanced Oil Recovery*, Elsevier, Amsterdam, 1981.
[13] S. B. Gorell and G. Homsy, *A theory of the optimal policy of oil recovery by secondary displacement processes*, SIAM J. Appl. Math., 43 (1983), pp. 79–98.

[14] H. S. Hele-Shaw, *On the motion of a viscous fluid between two parallel plates*, Trans R. Inst. Na. Archit. Lond., 40 (1898), pp. 18–.
[15] L. W. Lake, *Enhanced Oil Recovery*, Prentice Hall, Englewood Cliffs, NJ, 1989.
[16] W. Littman, *Polymer Flooding: Developments in Petroleum Science*, Elsevier, Amsterdam, 1998.
[17] N. Mungan, *Improved waterflooding through mobility control*, Canad. J. Chem. Engrg., 49 (1974), pp. 32–37.
[18] R. Needham and P. Doe, *Polymer flooding review*, J. Petroleum Technology, 12 (1987), pp. 1503–1507.
[19] J. Pearson, *The Stability of Some Variable Viscosity Flows with Application to Oil Extraction*, unpublished, Cambridge University Press, 1977.
[20] G. Pope, *The application of fractional flow theory to enhacned oil-recovery*, Soc. Pet. Eng. J., 20 (1980), pp. 191–205.
[21] G. Pope and W. Wade, *Lessons from enhanced oil recovery research for surfactant enhanced aquifer remediation*, in Surfactant-Enhanced Remediation of Subsurface Contamination, ACS Sympos. Ser. 594, American Chemical Society, Washington, DC, 1995, pp. 142–160.
[22] G. A. Pope and R. C. Nelson, *A chemical flooding compositional simulator*, Soc. Pet. Eng. J., 18 (1978), pp. 339–354.
[23] P. Saffman and G. Taylor, *The penetration of a fluid into a porous medium or Hele-Shaw cell containing a more viscous liquid*, Proc. Roy. Soc. London Ser. A, 245 (1958), pp. 312–329.
[24] D. Shah and R. Schecter, eds., *Improved Oil Recovery by Surfactants and Polymer Flooding*, Academic Press, New York, 1977.
[25] R. L. Slobod and J. S. Lestz, *Use of a graded viscosity zone to reduce fingering in miscible phase displacements*, Producers Monthly, 24 (1960), pp. 12–19.
[26] K. Sorbie, *Polymer-Improved Oil Recovery*, CRC Press, Boca Raton, FL, 1991.
[27] K. Taylor and H. Nasr-El-Din, *Water-soluble hydrophobically associating polymers for improved oil recovery: A literature review*, J. Pet. Sci. Eng., 19 (1998), pp. 265–280.
[28] A. Uzoigwe, F. Scanlon, and R. Jewett, *Improvement in polymer flooding: The programmed slug and the polymer-conserving agent*, J. Petrol. Tech., 26 (1974), pp. 33–41.
[29] J. Vargo, J. Turner, B. Vergnani, M. Pitts, K. Wyatt, H. Surkalo, and D. Patterson, *Alkaline-surfactant/polymer flooding of the Cambridge Minnelusa field*, SPE Res. Eval. Engrg., 3 (2000), 55663.
[30] L. Zerpaa, N. Queipoa, T. S. Pintosa, and J. Salagerb, *An optimization methodology of alkaline-surfactant-polymer flooding processes using field scale numerical simulation and multiple surrogates*, J. Pet. Sci. Eng., 47 (2005), pp. 197–208.
[31] Q. Zhijian, Z. Yigen, Z. Xiansong, and D. Jialin, *A successful ASP flooding pilot in Gudong oil field*, in Proceedings of the SPE/DOE Improved Oil Recovery Symposium, Society of Petroleum Engineers, Allen, TX, 1998, 39613-MS.
[32] Z. Zhijun and H. Yongmei, *Economic evaluation shows polymer flooding effectiveness*, Oil & Gas J., 21 (2002), pp. 56–59.